

Time Synchronization Error and Calibration in Integrated GPS/INS Systems

Weidong Ding, Jinling Wang, Yong Li, Peter Mumford, and Chris Rizos

The necessity for the precise time synchronization of measurement data from multiple sensors is widely recognized in the field of global positioning system/inertial navigation system (GPS/INS) integration. Having precise time synchronization is critical for achieving high data fusion performance. The limitations and advantages of various time synchronization scenarios and existing solutions are investigated in this paper. A criterion for evaluating synchronization accuracy requirements is derived on the basis of a comparison of the Kalman filter innovation series and the platform dynamics. An innovative time synchronization solution using a counter and two latching registers is proposed. The proposed solution has been implemented with off-the-shelf components and tested. The resolution and accuracy analysis shows that the proposed solution can achieve a time synchronization accuracy of 0.1 ms if INS can provide a hard-wired timing signal. A synchronization accuracy of 2 ms was achieved when the test system was used to synchronize a low-grade micro-electromechanical inertial measurement unit (IMU), which has only an RS-232 data output interface.

Keywords: GPS, INS, time synchronization, multi-sensor integration.

Manuscript received Nov. 20, 2006; revised Nov. 8, 2007.

This research is supported by the Australian Cooperative Research Centre for Spatial Information (CRC_SI) under project 1.3 'Integrated Positioning and Geo-referencing Platform'.

Weidong Ding (phone: +61 2 93854185, email: weidong.ding@unsw.edu.au), Jinling Wang (email: jinling.wang@unsw.edu.au), Yong Li (email: yong.li@unsw.edu.au), Peter Mumford (email: p.mumford@unsw.edu.au), and Chris Rizos (email: c.rizos@unsw.edu.au) are with the Satellite Navigation and Positioning Group, School of Surveying and Spatial Information Systems, University of New South Wales, Sydney, Australia.

I. Introduction

The global positioning system (GPS) receiver and inertial navigation system (INS) unit are two important sensors for providing position and attitude information for geo-referencing systems. A GPS/INS integrated system has many applications in surveying, remote sensing, mapping, and navigation. With optimal data fusion, the GPS could ensure long term geo-positioning accuracy and stability, while the INS could provide attitude information and partially mitigate against GPS signal outages.

Time synchronization between GPS and INS measurements is a common concern when implementing GPS/INS integrated systems. Since the GPS receiver and the INS unit are two separate (self-contained) subsystems, the clock difference and data transmission latency could cause data alignment discrepancies during the data fusion stage. Such alignment discrepancies may render the data fusion suboptimal. In some applications, the time synchronization of additional sensors, such as a barometer, odometer, or imaging sensor, might also be necessary.

The time synchronization issue has been extensively reported in research literature. The report on mobile multi-sensor systems by the International Association of Geodesy (IAG) working group [1] acknowledges its importance. A proposal for the IEEE inertial systems standard [2] suggests that the synchronization of the INS internal clock to an external time reference like the GPS clock is an important issue to be addressed.

In this paper, a detailed analysis of the limitations and advantages of different time synchronization scenarios and existing solutions is presented. A criterion for evaluating synchronization accuracy requirements is developed on the

basis of a comparison of the Kalman filter innovation series and the platform dynamics. An innovative time synchronization solution using a counter and two latching registers is proposed. The proposed solution is verified using a test system implemented with off-the-shelf components. Without an INS hard-wired timing signal, as reported in the test results, a synchronization accuracy of 2 ms was achieved when the test system was used to synchronize a low-grade INS sensor manufactured with micro-electromechanical systems (MEMS) technology, which has only an RS-232 data output interface.

II. Existing Solutions

The GPS time is typically used as a time reference for GPS/INS integrated systems. In addition to outputting positioning data and time messages through a serial data link, most GPS receivers provide a one pulse-per-second (PPS) electrical signal indicating the time of the turnover of each second. The alignment of the 1 PPS signal edge to standard GPS time is normally better than 1 μ s [3].

The inertial sensors used in GPS/INS integrated systems can be in the form of an inertial sensor assembly (ISA), inertial measurement unit (IMU), or inertial navigation system (INS) according to IEEE's definition. Depending on what information is extracted from them and their electrical interfaces, different time synchronization strategies may be employed.

1. Analog Interface

A successful implementation under this scenario is described in detail in [4] and [5], and is illustrated in Fig. 1. The GPS 1 PPS signal is used to trigger a 10 kHz 8-channel 16-bit analog-to-digital (A/D) converter in order to synchronize the starting time of every 10,000 samples to the GPS time. The A/D converter simultaneously samples the analog outputs from individual accelerometers, gyros and temperature sensors. The samples are averaged over 0.01 s and are sent for GPS/INS integration processing.

A similar solution is proposed by [6], in which a 0.4 ms synchronization accuracy is achieved using off-the-shelf components. The details concerning the construction of a synchronized A/D sampling circuit are given in [7]. Time synchronization implemented in A/D sampling circuits can be very precise (better than 1 μ s is possible). The coincidence of GPS and INS sampling at the turnover of each GPS second (assume a 1 Hz GPS data rate) eliminates the need for interpolation during data processing.

However, not all commercial INS sensors provide analog

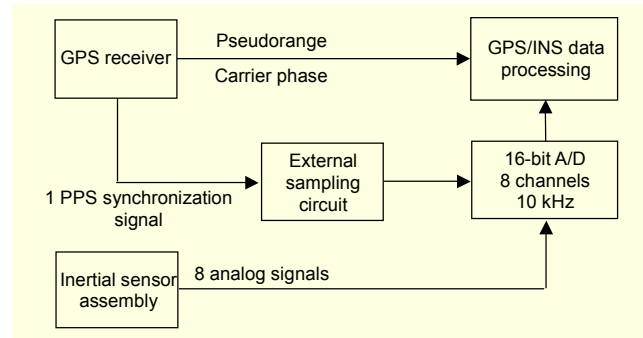


Fig. 1. Time synchronization scheme proposed in [5].

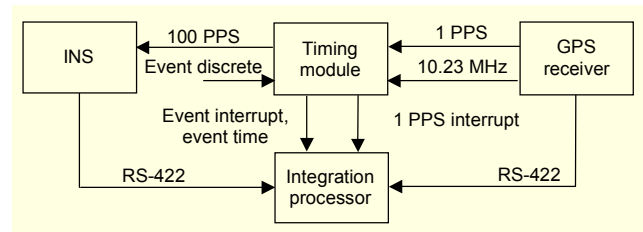


Fig. 2. Synchronization solution proposed in [8].

outputs. Adapting existing INS interfaces to the synchronized A/D sampling circuit is not a trivial task. Even if some manufacturers may provide INS sensors with analog outputs, as in the case of the Xbow IMU400CC, the output measurements normally go through an internal pre-processing procedure which includes A/D conversion, raw sampling data manipulation, and digital-to-analog conversions. The delays caused by those processes are hard to estimate.

Without using commercial INSs, individual inertial sensors are available on the market for building up proprietary INSs. However, their use is largely limited to lower end applications. This is because there are so many limiting factors preventing them from achieving a high performance. These possible factors include errors in mounting axes alignment, mounting base deformation, electrical circuit noise, and the lack of high precision calibrations using professional equipment. As will be discussed in section III, using a low grade INS might preclude the need to have the same time synchronization accuracy as would be needed for high grade INSs.

2. Digital Interface

Figure 2 shows a conceptual solution proposed in [8], in which an INS sensor has a digital data interface. The timing module is designed to accept the GPS 1 PPS signal and the 10.23 MHz signal, which is generated from the GPS P-code chipping rate. The timing module generates a synchronized 100 Hz PPS signal and passes it to the INS sensor. The sampling of inertial sensor measurements is synchronized to

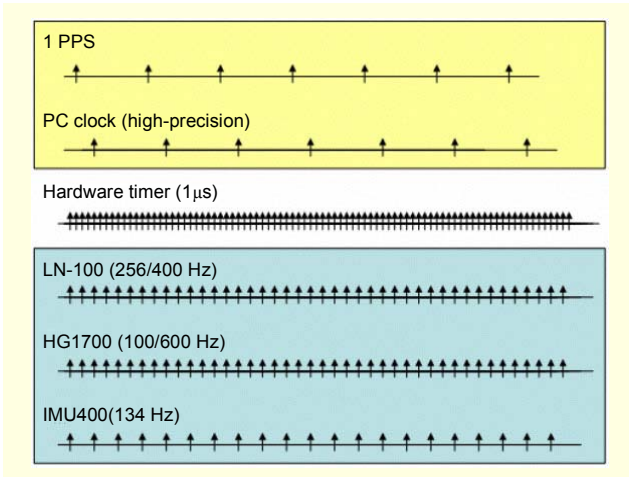


Fig. 3. Synchronization scheme introduced by [9]-[10].

this 100 Hz PPS signal. The 1 PPS signal is also introduced into the integration processor to define the beginning of each second. The INS data can thus be time-tagged according to GPS time received through an RS-422 link. The limitation of this solution is that the INS sensor has to be able to accept GPS PPS signals, which is very unlikely.

In [9] and [10], a successful implementation using the digital interface to synchronize the Litton LN100, Honeywell HG1700, and Xbow IMU400C (see Fig. 3) is described. In this scheme, the timing is accomplished by using the high precision PC clock as a common time base. A hardware timer which is running with 1 μ s resolution provides the link between the GPS time and the PC time. At every transition of the 1 PPS signal, the hardware saves a record. Through an interrupt, the software samples both the timer and the PC time and stores all the values for later processing. The transformation between GPS and PC time base is done in two steps: first, GPS vs. timer; then, PC vs. timer.

One limitation in using the digital interface is the necessity of data interpolation in order to make INS data coincide with GPS data in the Kalman filter measurement update. This is due to the asynchronous measurement sampling of the GPS and the INS sensors. When the INS sampling rate is 100 Hz and the GPS sampling rate is 1 Hz, a maximum misalignment of 5 ms can only be bridged using an interpolation technique.

Besides a digital interface, some INS sensors also output an electrical PPS signal to indicate the validation of the measurement data (similar to the 1 PPS generated by a GPS receiver). With the INS PPS signal, the INS internal pre-processing latencies can be determined and compensated.

When the INS sensor does not have a PPS signal output, the precise determination of the INS internal processing latency and communication latency is a challenge. Some software methods have been developed to estimate time synchronization errors in

data fusion algorithms [11]. Nevertheless, a hardware circuit is still necessary to provide initial data alignment; and the time synchronization accuracy is comparatively low in this case.

Due to the variety of possible time synchronization scenarios, there are some other non-typical solutions [12]-[14] applied under certain situations, which will not be detailed here.

III. Error Propagation

Considering a multivariable linear discrete system for the integrated GPS/INS system:

$$\begin{aligned} \mathbf{x}_k &= \Phi_{k-1} \mathbf{x}_{k-1} + \mathbf{w}_{k-1}, \\ \mathbf{z}_k &= \mathbf{H}_k \mathbf{x}_k + \mathbf{v}_k, \end{aligned} \quad (1)$$

where \mathbf{x}_k is ($n \times 1$) state vector, Φ_k is ($n \times n$) transition matrix, \mathbf{z}_k is ($r \times 1$) observation vector, \mathbf{H}_k is ($r \times n$) observation matrix, and \mathbf{w}_k and \mathbf{v}_k are uncorrelated white Gaussian noise sequence with means and covariances:

$$\begin{aligned} E(\mathbf{w}_k) &= E(\mathbf{v}_k) = 0, \\ E(\mathbf{w}_k \mathbf{v}_i^T) &= 0, \\ E(\mathbf{w}_k \mathbf{w}_i^T) &= \begin{cases} \mathbf{Q}_k, & i = k, \\ 0, & i \neq k, \end{cases} \\ E(\mathbf{v}_k \mathbf{v}_i^T) &= \begin{cases} \mathbf{R}_k, & i = k, \\ 0, & i \neq k, \end{cases} \end{aligned} \quad (2)$$

where $E\{\cdot\}$ denotes the expectation function, and \mathbf{Q}_k and \mathbf{R}_k are the covariance matrix of process noise and observation errors, respectively. The KF state prediction and state covariance prediction are given as

$$\begin{aligned} \hat{\mathbf{x}}_k &= \Phi_{k-1} \hat{\mathbf{x}}_{k-1}, \\ \hat{\mathbf{P}}_k^- &= \Phi_{k-1} \hat{\mathbf{P}}_{k-1} \Phi_{k-1}^T + \mathbf{Q}_{k-1}. \end{aligned} \quad (3)$$

The Kalman measurement update algorithms are given as

$$\begin{aligned} \mathbf{K}_k &= \hat{\mathbf{P}}_k^- \mathbf{H}_k^T (\mathbf{H}_k \hat{\mathbf{P}}_k^- \mathbf{H}_k^T + \mathbf{R}_k)^{-1}, \\ \hat{\mathbf{x}}_k &= \hat{\mathbf{x}}_k^- + \mathbf{K}_k (\mathbf{z}_k - \mathbf{H}_k \hat{\mathbf{x}}_k^-), \\ \hat{\mathbf{P}}_k &= (\mathbf{I} - \mathbf{K}_k \mathbf{H}_k) \hat{\mathbf{P}}_k^-, \end{aligned} \quad (4)$$

where \mathbf{K}_k is the Kalman gain, which defines the updating weight between new measurements and predictions from the system dynamic model.

The growth of many errors in the horizontal channels of a Schuler-tuned INS is bounded by the Schuler tuning effects, while the errors in the vertical channels tend to grow exponentially with time. To deal with the large INS navigation errors and modelling non linearities, the actual implementation of the Kalman filter in GPS/INS integration is often in the

complementary form [15]. In such configurations, the observation vector in (1) is the difference between the GPS measurements and INS measurements. When expressed in the continuous time domain, the observation vector $\mathbf{z}(t)$ is given as

$$\begin{aligned}\mathbf{z}(t) &= \mathbf{r}_{GPS}(t) - \mathbf{r}_{INS}(t) \\ &= \mathbf{r}_{GPS}(t) - \left(\mathbf{r}_{INS}(0) + \int \mathbf{v}_{INS}(0) + \iint \mathbf{a}(t) \right),\end{aligned}\quad (5)$$

where $\mathbf{r}_{GPS}(t)$ is the GPS position measurements, $\mathbf{r}_{INS}(0)$ and $\mathbf{v}_{INS}(0)$ are the INS initial position and velocity and $\mathbf{a}(t)$ is the acceleration measured by INS sensors under the proper coordinate frame. The integration symbol \int represents the integration within one GPS sampling period. Assuming that the INS initial position and velocity are known, if there are time synchronization errors in the INS measurements, the observation vector is changed to $\tilde{\mathbf{z}}(t)$:

$$\tilde{\mathbf{z}}(t) = \mathbf{r}_{GPS}(t) - \left(\mathbf{r}_{INS}(0) + \int \mathbf{v}_{INS}(0) + \iint \mathbf{a}(t + \Delta t) \right), \quad (6)$$

where Δt denotes the INS time synchronization error, which can either be positive or negative. It can be treated as a constant in the following discussion. After taking a Taylor expansion to the INS measurements, $\tilde{\mathbf{z}}(t)$ becomes

$$\begin{aligned}\tilde{\mathbf{z}}(t) &= \mathbf{r}_{GPS}(t) - \left(\mathbf{r}_{INS}(0) + \int \mathbf{v}_{INS}(0) + \iint \mathbf{a}(t) + \iint (\mathbf{a}'(t) \Delta t) \right) \\ &= \mathbf{z}(t) - \iint (\mathbf{a}'(t) \Delta t) \\ &= \mathbf{z}(t) - \boldsymbol{\zeta}.\end{aligned}\quad (7)$$

It is clear from (7) that the time synchronization error of the INS measurements introduces an additional observation error, $\boldsymbol{\zeta}$. The magnitude of this error is dependent on the delay time Δt and the change of the vehicle acceleration $\mathbf{a}'(t)$ (also called jerk) which represents the dynamics. The impact of this error on the Kalman filtering process can be evaluated using (4). Considering the INS synchronization errors, the measurement update becomes

$$\tilde{\mathbf{x}}_k = \hat{\mathbf{x}}_k^- + \mathbf{K}_k \left(\mathbf{z}_k - \boldsymbol{\zeta}_k - \mathbf{H}_k \hat{\mathbf{x}}_k^- \right). \quad (8)$$

The state estimation errors caused by $\boldsymbol{\zeta}$ at each epoch are given as

$$\boldsymbol{\varepsilon} = \tilde{\mathbf{x}}_k - \hat{\mathbf{x}}_k = -\mathbf{K}_k \boldsymbol{\zeta}_k. \quad (9)$$

This implies that the observation error $\boldsymbol{\zeta}_k$ is distributed to individual state estimates according to the Kalman gain matrix. In each measurement update, this error distribution is largely dependent on the observation geometry \mathbf{H}_k . Due to the temporal filtering effect of the Kalman filter, the white and Gaussian elements of the error $\boldsymbol{\varepsilon}$ would be damped out as the filtering process becomes stabilised. The non-white and non-

Gaussian part would remain as an estimation bias.

The impact of the synchronization error can be numerically analysed by adding intentional time delays to INS data and investigating their influence on the integration results. When different increments of time delay are added, the positioning errors steadily increase as the time delay becomes larger. The same trend is observed when the magnitude of the time delay becomes negative, which is the case when the INS clock bias is negative. More detailed results are presented in [16].

In general, the time synchronization accuracy required by the integrated GPS/INS system can be evaluated using (8). If

$$|\boldsymbol{\zeta}_k| \ll \left| \mathbf{z}_k - \mathbf{H}_k \hat{\mathbf{x}}_k^- \right|, \quad (10)$$

then the estimation errors caused by the INS data latency can be omitted. From (10) and (7), we can derive

$$|\Delta t| \ll \frac{\left| \mathbf{z}_k - \mathbf{H}_k \hat{\mathbf{x}}_k^- \right|}{\left| \iint \mathbf{a}'(t) \right|}. \quad (11)$$

Some conclusions can be drawn from (11). First, the required time synchronization accuracy is negatively proportional to the magnitude of the Kalman filter innovations, which is largely dependent on INS accuracy and how well it is calibrated. Because a higher grade INS will result in smaller innovation magnitude, higher time synchronization accuracy is required when the INS is to be calibrated using GPS measurements. In contrast, lower time synchronization accuracy is sufficient when using low grade INS sensors. Second, the required time synchronization accuracy is positively proportional to the magnitude of the vehicle dynamics. Higher time synchronization accuracy is required for high dynamic applications.

Precise calculation of the required Δt using (11) may not be possible when considering the simplification in derivation, and the impact of the errors from INS accelerometers, gyroscopes, and the gravity model. However, a rough estimation can still be given. Suppose a GPS/INS integrated system can have an acceleration change of 9.8 m/s^3 (jerk), and the GPS updating rate is 1 Hz. Double integration of the jerk value generates a speed of about 5 m/s. When the innovation RMS is about 5 cm, in order to make the right side value ten times larger than the left side value in (11), the required time synchronization accuracy should be set to 1 ms.

IV. Proposed Method

Based on the analysis of the synchronization scenarios and requirements, we propose three steps to solve the time synchronization problem:

- Build up a cross link between the GPS and INS time axes.

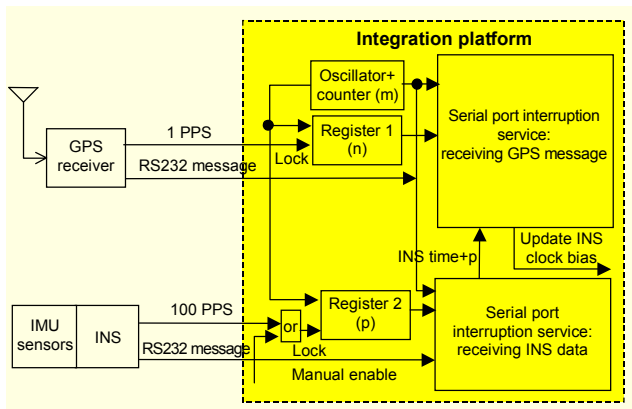


Fig. 4. Proposed time synchronization design.

- Correct the INS time-tag errors.
- Interpolate INS data to ensure that the INS and GPS measurements coincide at each epoch.

Figure 4 illustrates the proposed time synchronization system that comprises a GPS receiver, an INS sensor and one integration platform. The integration platform can either be a personal computer (PC), or an embedded processor board. Both the GPS receiver and the INS sensor have two connections to the integration platform, namely, one serial data link and one electrical PPS signal connection.

On the integration platform a series of 100 kHz ticking pulses are generated by a stable source and are counted by a 24-bit counter. The leading edge of the GPS 1 PPS signal and the INS PPS timing mark trigger the corresponding register to latch the counter. The registers store the value until the next trigger signal comes. The time difference between the GPS 1 PPS signal and the INS time mark can be calculated by comparing the values of the two registers.

During the triggering intervals, the stored values in the register are picked up by the serial port interrupt services when their corresponding serial messages are received. Hence the received messages can be tagged with the latched counter values. By referring to those counter values, a link between GPS time and INS time messages can be established.

When the INS PPS timing mark is not available, the manual enable (which could be a hardware or software switch) shown in Fig. 4 must be used to set the register into pass-through mode. In this way, the INS register reading corresponds to the arrival time of the INS message.

When the INS can send a PPS timing mark to the integration platform (as in Fig. 4), the true time of the INS PPS signals can be calculated as

$$INS_PPS_true_time_l = GPS_time_sec_k + \frac{p_l - n_k}{n_k - n_{k-1}}, \quad (12)$$

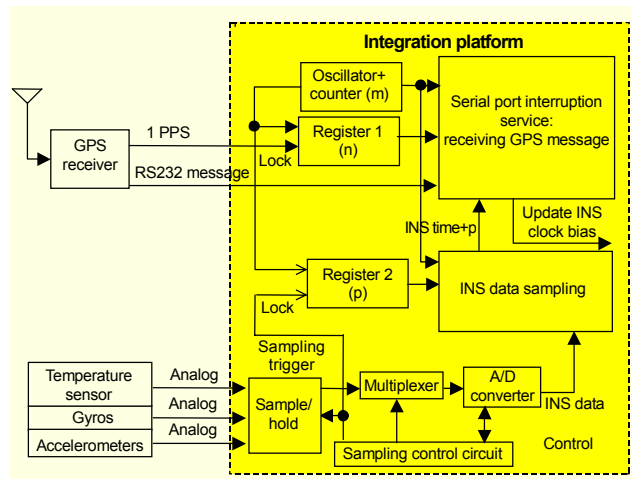


Fig. 5. Time synchronization with analog INS inputs.

where k and l denote the latest GPS and INS sampling epochs, respectively; and n and p denote the readings of the GPS register and INS register, respectively. Thus, the INS internal clock bias can be calculated as

$$INS_time_bias = INS_PPS_time - INS_PPS_true_time. \quad (13)$$

This calculated INS time bias is used to calibrate the INS data time-tags.

When an INS PPS timing mark is not available, the time that the INS register's value represents is the INS message arrival time. Hence, the INS register readings include additional delays, including the INS data processing delay and serial communication delay, which have to be extracted. Precise determination of the magnitude of these additional delays is quite challenging. The INS manufacturer can provide it as a constant parameter, or the parameter can be evaluated experimentally, which is the method adopted in this study, which will be demonstrated in the following sections.

With correct time-tags, the raw INS data can be easily interpolated to the points that exactly coincide with the GPS measurements. The interpolation can be linear, quadratic, or cubic, depending on the accuracy required. The interpolation algorithm can be implemented in an extended Kalman filter (EKF) time update process.

When the proposed method involves interfacing with the INS analog outputs, an A/D conversion circuit needs to be added to the integration platform. The trigger signal of the A/D circuit can be used to trigger the INS latching register, as indicated in Fig. 5.

V. Implementation

To verify the feasibility of the proposed time synchronization

method, a data logging system was implemented using off-the-shelf components, including a notebook PC, Windows operating system, data acquisition card (DAQ), and the LabView software package from National Instruments (NI).

The DAQ card is a low-cost E series multifunction PCMCIA card. It has two 24-bit counters and one 100 kHz internal pulse source. A simple LabView application was developed to handle the data received from the two EIA-232 ports, that is, one for receiving GPS data and one for receiving INS data.

VI. Field Test

The field test used two Leica System 530 GPS receivers, one Jupiter GPS receiver, a BEI C-MIGITS II INS system, and one Crossbow IMU400C IMU. One Leica GPS receiver was set up as a reference station, and the other one was set up on the roof of the test vehicle, together with the INS and IMU units. The C-MIGITS II was closely fastened to the top of the IMU400C so that their dynamics would be the same during the vehicle test.

The GPS data from the Jupiter GPS receiver and the raw IMU data from the Crossbow IMU400C were time synchronized and logged using the time synchronization system described in sections IV and V, and stored on the notebook PC for post-processing. The data collected from the two Leica GPS receivers and the C-MIGITS II was used to calculate the reference trajectory.

VII. Test and Result

1. Measurement of Periodic Timing Signals

In this test the time synchronization system was used to measure GPS 1 PPS intervals. Since the GPS 1 PPS timing mark is strictly aligned to the GPS second to within $\pm 1 \mu\text{s}$ [17], the 1 PPS interval is effectively 1 s. With a 100 kHz ticking frequency, the counting value during each 1 PPS interval should be 100,000. Repeated tests showed that the actual counting values were either 100,000 or 100,000-1, which is equivalent to 0.01 ms timing accuracy.

2. Measurement of Two Consecutive Timing Signals

In this test, the source signals were the GPS 1 PPS timing pulse and a signal generated by delaying the GPS 1 PPS for pre-defined time intervals. These time intervals were controlled in increments of about $20 \mu\text{s}$. The shortest time interval was $25 \pm 10 \mu\text{s}$. The two source signals were precisely monitored using a digital oscilloscope with a timing accuracy better than $1 \mu\text{s}$. Figure 6 is a snapshot of the oscilloscope display. The blue line is the original GPS 1 PPS signal, and the black line is the

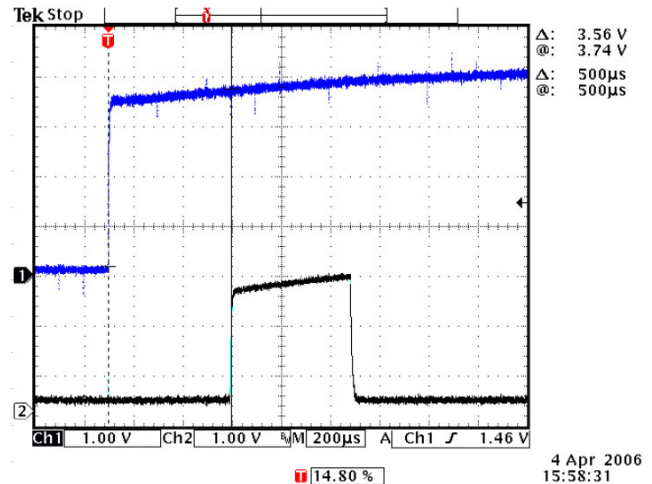


Fig. 6. Oscilloscope image showing the time interval between the rising edges of two signals.

generated signal. The time interval between the rising edges of the two signals is the delay time monitored using the oscilloscope. The same delay time was measured simultaneously using the implemented time synchronization system.

Comparison of the two results indicates that for every 0.1 ms change of the delay time in the range of 0.1 ms to 0.9 ms, the corresponding counting values changed 10 ± 2 (with a 100 kHz ticking frequency). So the counting accuracy can be converted into a timing accuracy of 0.02 ms. We conservatively estimate the timing accuracy of the implemented circuit to be better than 0.1 ms.

3. Correlation Check

The C-MIGITS II is a tightly-integrated GPS/INS system comprising a digital quartz inertial unit, a navigation processing unit, and a GPS receiver. With the aid of the GPS receiver, the internal time of the C-MIGITS II is precisely synchronized to GPS time. Through a serial port, the C-MIGITS II can output precisely time-tagged IMU raw measurements at a 100 Hz data rate. The performance of the C-MIGITS II and the Xbow IMU400C is compared in Table 1.

The IMU400C data was time synchronized and logged using the implemented time synchronization system. Some of the IMU400C accelerometer measurements and the C-MIGITS II reference accelerometer data of the x-axis have

Table 1. C-MIGITS II and Xbow IMU400C technical specifications.

	C-MIGITS II	Xbow IMU400C
Accelerometer bias	500 μg	8.5 mg
Gyro bias	5 deg/h	1 deg/s

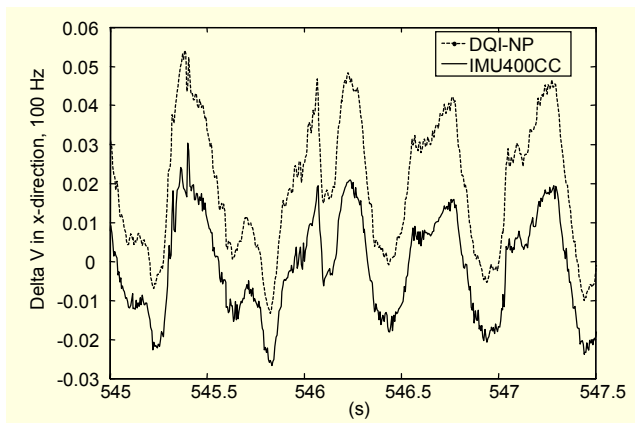


Fig. 7. Comparison between recorded IMU400C raw data and C-MIGITS II data Delta V in x-direction.

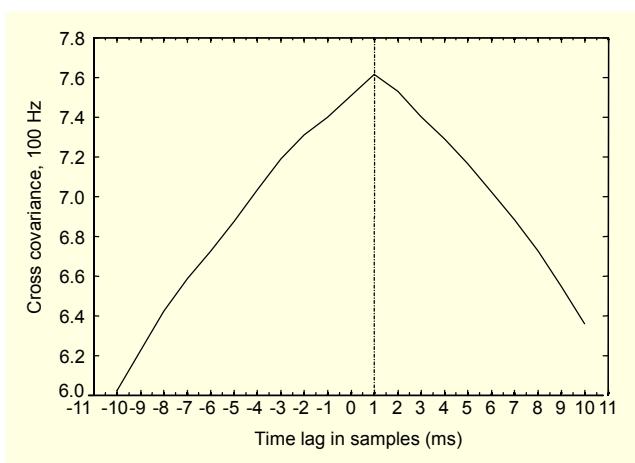


Fig. 8. Check of Xbow and C-MIGITS II data consistency using the correlation method.

been plotted in Fig. 7. Plots of other measurements have a similar appearance.

Figure 7 demonstrates that the two recorded results coincide with each other very well. To examine the consistency in detail, a cross covariance check of the two data streams was carried out using MATLAB tools. If the two data streams are fully synchronized, the cross covariance peak should appear where the time-lag equals zero. Figure 8 shows the results of comparing the IMU400CC raw accelerometer x-direction data and the corresponding C-MIGITS II reference data before applying time synchronization corrections. The peak value of the cross covariance appears when the lag equals one, which means the C-MIGITS II data is leading the IMU400C data by approximately one sampling period. The equivalent time difference is about 10 ms when the data sampling rate is 100 Hz.

The comparison of time synchronization accuracy using the cross covariance method was limited by the data sampling frequency, which is 100 Hz. Alternatively, we investigated the consistency of the two data streams using the cross-correlation

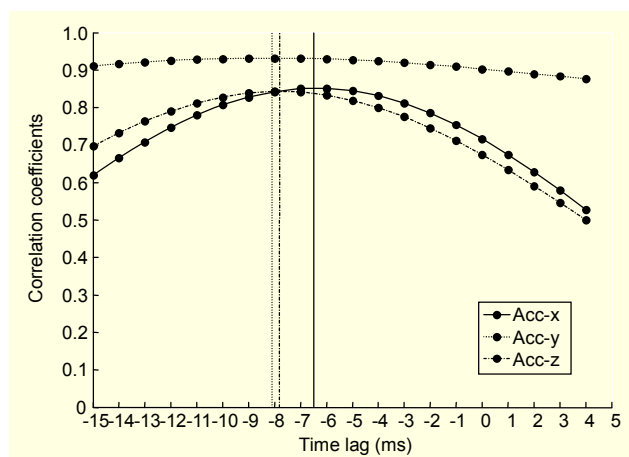


Fig. 9. Cross-coefficients between C-MIGITS II data and IMU400C data.

coefficients method. The cross-correlation coefficient of the two independent data series is a normalised coefficient value which represents the degree of similarity between the two data series. The cross-correlation coefficient equals one when the two data series exactly repeat each other.

The advantage of using the cross-correlation coefficient method is that several data series can be generated from the objective data set by shifting time tags by 1 ms each time and then treated as independent data series to be compared with the reference data. The most similar data sets would have the highest cross-correlation coefficient value. By examining the time lag where the highest cross-correlation coefficient appears, the timing difference between the two data sets can be found and can be used for time synchronization compensation. Figure 9 shows the results of this comparison. A 7.5 ms average latency of IMU400CC data is observed from repeated tests. According to the manufacturer's technical specification [18], the IMU400CC has a data latency of about 6.4 ms. Considering the platform processing time, the 7.5 ms total time delay is reasonable.

Overall, the time synchronization accuracy of this field test was limited by the fact that the Xbow IMU400CC does not provide precise information about the internal processing delay, neither through an instantaneous analog output nor via PPS timing marks. The synchronization accuracy in this case is estimated to be at the level of 2 ms based on the distribution of the cross-correlation coefficient peaks. However, the synchronization accuracy of the proposed hardware circuit was demonstrated in tests 1 and 2 to be at the level of 0.1 ms. Since the typical vehicle jerk for a passenger car is below 0.01 m/s^3 and may be up to 4 m/s^3 during emergency break manoeuvres [19], a synchronization accuracy of 2 ms is translated to a maximum 4 mm observation error according to (7), which is sufficient for general ground vehicle applications.

VIII. Concluding Remarks

Depending on the requirements of the integration performance and the type of INS sensor used in GPS/INS integration, different time synchronization strategies should be applied. Practical limitations of sensor types and interfaces influence the choice of time synchronization solutions, and the synchronization accuracy that can in fact be achieved.

To find the optimal time synchronization solution for a particular GPS/INS integration application, the required time synchronization accuracy must first be evaluated properly. This paper proposed an algorithm to analyse the impact of data latency on Kalman filter measurement updates and to determine the synchronization accuracy that should be satisfied.

An innovative time synchronization solution, which is simple and flexible for implementation, was proposed and tested using a low-grade MEMS IMU sensor. A time synchronization accuracy of about 2 ms was reached, which is limited by the nature of the sensor and the interface type. Nevertheless, the feasibility of the proposed solution has been verified.

Although this study is concerned with the integration of GPS and INS, the principles are equally applicable when additional imaging and navigation sensors are involved.

References

- [1] N. El-Sheimy, "Mobile Multi-Sensor Systems Final Report (1995-1999)," International Association of Geodesy, 1999. http://www.gfy.ku.dk/~iag/Travaux_99/sc4wg1.htm. (accessed June 2006)
- [2] R.K. Curey, M.E. Ash, L.O. Thielman, and C.H. Barker, "Proposed IEEE Inertial Systems Terminology Standard and Other Inertial Sensor Standards," *IEEE Position Location Navigation Symp.*, Monterey, California, USA, Apr. 2004, pp. 426-432.
- [3] P.J. Mumford, "Timing Characteristics of the 1 PPS Output Pulse of Three GPS Receivers," *6th Int. Symp. on Satellite Navigation Technology Including Mobile Positioning & Location Services*, Melbourne, Australia, July 2003, p. 45.
- [4] J.L. Farrell, "GPS for Avionics Synchronization," *ION GPS*, Salt Lake City, Utah, USA, Sept. 2001, pp. 3149-3152.
- [5] F. van Grass and J.L. Farrell, "GPS/INS: A Very Different Way," *ION 57th Annual Meeting*, Albuquerque, New Mexico, USA, June 2001, pp. 715-721.
- [6] B. Li, "A Cost Effective Synchronization System for Multisensor Integration," *ION GNSS*, Long Beach, California, USA, Sept. 2004, pp. 1627-1635.
- [7] Y.F. Ma, B.L. Zhou, Z.G. Wan, and L.Y. Zhao, "Data Synchronization and Fusion Method in MIMU/GPS Integration Navigation System," *Journal of Chinese Inertial Technology*, vol. 12, no. 3, 2004, pp. 28-31.
- [8] D. Knight, "Achieving Modularity with Tightly-Coupled GPS/INS," *IEEE Plans*, Monterey, California, USA, Mar. 1992, pp. 426-432.
- [9] D.A. Grejner-Brzezinska, "Integrated Systems for Mobile Mapping," Workshop presented at the University of New South Wales, Sydney, Australia, 13-14 Dec. 2004.
- [10] C. Toth, D.A. Grjner-Brzezinska, "Performance Analysis of the Airborne Integrated Mapping System (AIMSTM)," *ISPRS Comm. II Symp. on Data Integration: Systems and Techniques*, Cambridge, England, 1998, pp. 320-326.
- [11] H.K. Lee, J.G. Lee, and G.I. Jee, "Calibration of Measurement Delay in Global Positioning System/Strapdown Inertial Navigation System," *Journal of Guidance, Control, and Dynamics*, vol. 25, no. 2, 2002, pp. 240-247.
- [12] T.J. Ford, J.B. Neumann, and I. Williamson, "Inertial GPS Navigation System," U.S. Patent, 6721657 B2, 2004.
- [13] R.W. Petrie and P.R. Walton, *Determining Time Stamps in a Data Acquisition System*, U.S. Patent, US 6574244 B1, 2003.
- [14] R.F. Varley and J.J. Maney, *Hybrid GPS/ Inertially Aided Platform Stabilization System*, U.S. Patent, 6122595, 2000.
- [15] R.G. Brown and P.Y.C. Hwang, *Introduction to Random Signals and Applied Kalman Filtering*, New York, John Wiley & Sons, 1997.
- [16] W. Ding, J. Wang, P. Mumford, Y. Li, and C. Rizos, "Time Synchronization Design for Integrated Positioning and Georeferencing Systems," *Proc. SSC, Spatial Intelligence, Innovation, and Praxis*, Melbourne, Australia, Sept. 2005, pp. 1265-1274.
- [17] Rockwell, *Jupiter Global Positioning System (GPS) Receiver (part no. TU30-D140-141/151)*, Newport Beach, Rockwell Semiconductor Systems, 1997.
- [18] Crossbow, *DMU User's Manual*, USA, Crossbow Technology, Inc., 2002.
- [19] A. Wieser, *GPS-Based Velocity Estimation and Its Application to an Odometer*, Shaker-Verlag, Aachen, 2007.



Weidong Ding is currently a PhD student with the School of Surveying and Spatial Information Systems, at the University of New South Wales, Sydney, Australia. He received his BE in electrical engineering from Beijing Polytechnic University, China, and his ME in electrical engineering from the University of New South Wales, Australia. His research is focused on developing an integrated positioning and geo-referencing platform for mobile mapping and navigation applications.



Jinling Wang is a senior lecturer with the School of Surveying & Spatial Information Systems, University of New South Wales. He is a Fellow of the Royal Institute of Navigation, UK, and a Fellow of the International Association (IAG) of Geodesy. Jinling is a member of the Editorial Board for the international journal GPS Solutions, and Chairman of the study group (2003-2007) on pseudolite applications in positioning and navigation within the IAG's Commission 4. He was 2004 President of the International Association of Chinese Professionals in Global Positioning Systems (CPGPS). Jinling holds a PhD in GPS/Geodesy from the Curtin University of Technology, Australia.



Yong Li, PhD, is a senior research fellow at the Satellite Navigation and Positioning (SNAP) Lab within the School of Surveying & Spatial Information Systems, the University of New South Wales, Sydney, Australia. He was involved in development of a spaceborne GPS attitude determination receiver, a MEMS inertial sensors/GPS system for a sport application, and a field programmable gate array- (FPGA-) based real-time GPS/INS integrated system. His current interests include integration of GPS, INS, and pseudolite (Locata), attitude determination, GPS receiver technique, FPGA technology, and its application to navigation, and optimal estimation/filtering theory and applications.



Peter Mumford is a research assistant in the Satellite Navigation and Positioning group (SNAP), at the School of Surveying and Spatial Information Systems, University of New South Wales, Sydney Australia. Currently he is working on GNSS receiver design and INS/GNSS integration. Peter has an engineering degree in surveying, and a science degree in mathematics. He specializes in FPGA design, software, RF and electronic design.



Chris Rizos is a graduate of The University of New South Wales (UNSW), Sydney, Australia; obtaining a PhD in satellite geodesy in 1980. Chris is currently the head of the School of Surveying and Spatial Information Systems at UNSW. Chris has been researching the technology and high precision applications of GPS since 1985, and established over a decade ago the Satellite Navigation and Positioning group at UNSW, today the largest academic GPS and wireless location technology R&D laboratory in Australia (<http://www.gmat.unsw.edu.au/snap>). Chris is the Vice President of the International Association of Geodesy (IAG), a member of the IAG/IHO's Advisory Board on the Law of the Sea, a member of the Governing Board of the International GNSS Service, and a member of the IAG's Global Geodetic Observing System Steering Committee. Chris is a Fellow of the IAG and the Australian Institute of Navigation.